

Observing Astronomical Redshift Through Optical Red and Blue Slope Filters

Matthew J. McNeff

A senior thesis submitted to the faculty of
Brigham Young University
in partial fulfillment of the requirements for the degree of
Bachelor of Science

J. Ward Moody, Advisor

Department of Physics and Astronomy

Brigham Young University

August 2014

Copyright © 2014 Matthew J. McNeff

All Rights Reserved

ABSTRACT

Observing Astronomical Redshift Through Optical Red and Blue Slope Filters

Matthew J. McNeff
Department of Physics and Astronomy
Bachelor of Science

[We developed and employed a new method for determining the redshift of galaxies between the range of 2000 cz to 10,000 cz. The method involved getting a transmission through sloped blue and red filters, along with a continuum filter. The Moody-Holden-McNeff Relation is detailed, giving the relationship between the transmissions through the filters and the estimated redshift. The data that was collected for 5 nights is outlined along with the 3 different methods of analysis. Despite the fact that the data was cloudy and often had low signal to noise, there is good evidence that the method worked and deserves follow up research. The next step will be to ensure the data is taken on photometric nights.]

Keywords: Redshift, Galaxy Distance, Slope Filters

ACKNOWLEDGMENTS

[I would first like to acknowledge Dr. J. Ward Moody for the idea and his continual support throughout the project. I would also like to thank Marcus Holden, Angel Ritter, and Chuck Honick for their hard work in helping me reduce the data and brainstorm ideas. I would like to thank Dan McNeff for supporting me with work and housing throughout my undergraduate carrer. Also thanks to Mariann Adams and Evelyn McNeff for help with the editing, and most of all I would like to thank my wife Karen for her help, and her patience with my many late nights and stress, and to the Lord for helping me to reach beyond my abilities and finish this work.]

Contents

Table of Contents	iv
1 Introduction	1
1.1 Redshift	1
1.2 Ramp Filters	3
1.3 Redshift Fitting Model	8
2 Observing and Implementation	10
2.1 Instrumentation	10
2.2 Targets	12
2.3 Observing	13
2.4 Data Reduction	14
3 Results	16
3.1 Data	16
3.2 Fit Vs. Real CZ	20
3.2.1 Straight Count Averages	20
3.2.2 Noise Revision	24
3.2.3 Changing the Continuum	28
3.2.4 Other Continuum	33
3.2.5 Closest Point Method	34
4 Conclusions	36
4.1 Discussion	36
4.2 Future Work	37
Bibliography	39

Chapter 1

Introduction

1.1 Redshift

Since the dawn of man we have looked at the heavens and marveled. We have wondered what the stars are made of, what role they play in our existence, and of course how far away they are. Over the centuries our understanding of the heavens has greatly improved. We believe that we understand what stars are made of, and we know that they play a vital role in seeding the universe with the material it takes to build everything - including ourselves. We have also devised a myriad of clever means of determining the distances to the stars. Beginning with the observations of parallax for nearby stars, down to the modern-day detections of supernova and variable stars in distant galaxies, we have a host of methods available to us to help us determine how large our universe really is.

As we continue to go further and further into the universe, it becomes less useful to measure in terms of the distance between the earth and the sun, light years, or even parsecs. The more distant we continue to go, the more we need a larger and larger measuring stick. When we get out into the

regime of very distant galaxies, it becomes helpful to speak of the distances in terms of redshift, which is a shifting of frequency toward redder values. Frequency shift is a phenomenon that occurs in all waves as the source propagating the wave is moving relative to the observer. The most familiar example of this would be the doppler shift of sound waves (think ambulance driving by), but the same principle applies to light waves. As a light source is moving away from an observer, the frequency of light is shifted towards the less energetic or "red" side of the spectrum. Hence as a light source is moving away from us we see a "red-shift."

Our current understanding of the Universe is that it is expanding in all directions, so everything that is not gravitationally bound is spreading apart, moving away from each other. This was first discovered by Edwin Hubble as he did his groundbreaking research on galactic distances. Hubble determined that there was a linear relationship between how far away a galaxy was and how fast it was moving away from us. The rate at which they are moving apart is called the Hubble constant, and the relationship is the speed of light multiplied by the redshift is equal to the distance to the galaxy multiplied by the Hubble constant (Ryden & Peterson 2010). The further the galaxy was from us, the faster it was moving away, and hence the larger the redshift observed. Thus we can use redshift as a fairly reliable estimate for distance from and between distant galaxies.

Normally redshift is determined through careful spectroscopy work, where one will look for certain characteristic chemical lines, such as oxygen III or hydrogen, and will measure how far they are shifted from laboratory produced stationary spectra. Redshift is usually represented by the letter "z" and is a unitless ratio of the change in the frequency divided by the original frequency

$$z = \frac{\lambda_{new} - \lambda_{normal}}{\lambda_{normal}} \quad (1.1)$$

with normal values being between 0 and 0.1. Recent observations of the Hubble Deep Field have revealed several galaxies with redshifts in excess of 8.5, and one possible candidate with a redshift

of 11.9 (R. Ellis 2013), which is about as far as we can go with current instrumentation. For less extreme redshifts it is common to express the distance as the redshift multiplied by the speed of light cz , with common values of 100 to 100,000.

Modern day spectroscopy is a much more precise science than it was in the days of Edwin Hubble. We often use spectrographs with blazed (multi-directionally cut), or holographically cut surfaces (S.Barden et al. 1988). While these instruments are very accurate, just like any precision optics they are very delicate and can be cumbersome. The main problem involved in doing redshift work is that it requires large telescopes in order to gather enough light to make the measurements. The cost of building such telescopes is often beyond the means of researchers, and the demand for time on the ones currently existing mean they have to be very selective on the projects they take on. Consequently, our research focused on finding an inexpensive and robust method for accurately measuring the redshift of distant objects without having to use a large telescope.

The ultimate purpose of the method is to see if it can be employed in a dedicated survey of galactic voids using a small telescopes like the 16" R.O.V.O.R. telescope in Delta, Utah currently operated by Brigham Young University (J. Moody 2012). The method would need to be employable with the least amount of human interaction possible, as the telescope is controlled remotely, 90 miles away from BYU campus.

1.2 Ramp Filters

An idea put forth by Dr. J. Ward Moody in the fall of 2013 was to try to find some way of measuring the light of a given galaxy through a set of optical filters, then correlate those measurements with their known redshifts to find some sort of relationship. The idea of using narrow band optical

filters to help determine the location of a galaxy had previously been employed by J. Moody, C. Draper, S. McNeil and M. Joner using the Mayall 4-meter telescope on Kitt Peak to study several voids (Moody Provo, UT, Nov. 2013). Their method was to use three 60\AA FWHM redshifted $H\alpha$ filters, each offset by 35\AA so that they overlapped.

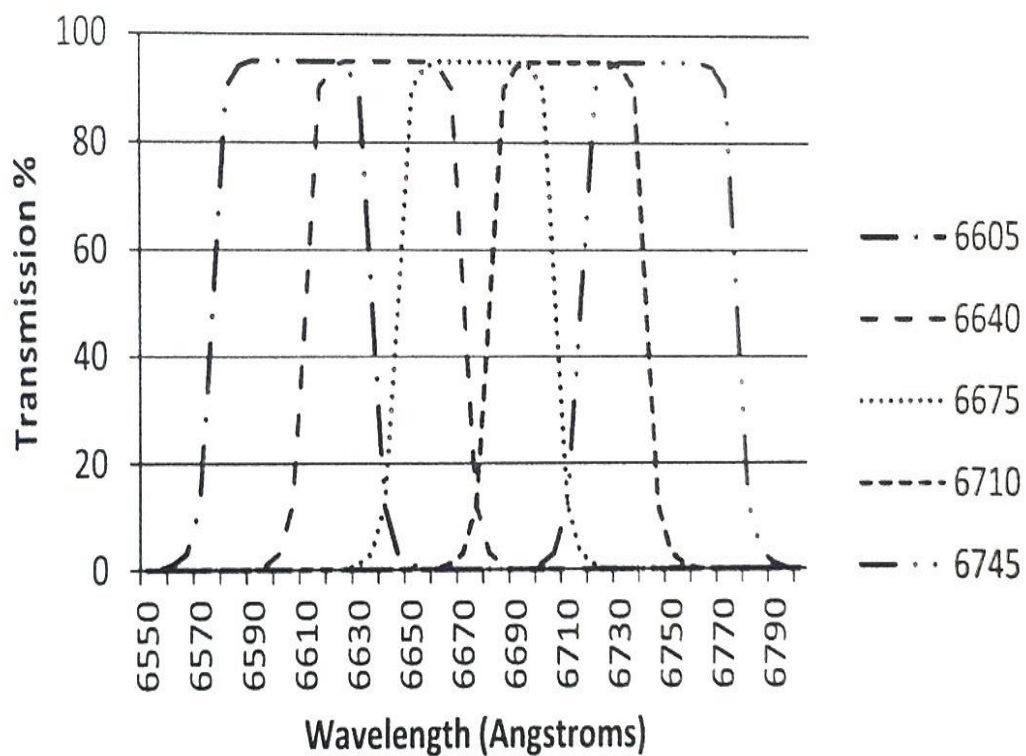


Figure 1.1 The transmission curves suggested by Moody et al to use in probing voids for emission-line galaxies. In practice only the middle three filters were used. (Moody Provo, UT, Sept. 2013).

In theory, spacing the filters 35\AA apart creates an overlap of the sloped transmission region from the 0% to 90% transmission of one filter into its two neighbors, leaving no gaps in the set. In this way every candidate object will have the $H\alpha$ wavelength detected in the 90% region one of the filters and, depending on its redshift, also in the wings of one of its neighbors. By comparing the relative intensities of the object in both filters, Dr. Moody and the others theorized they could determine the $H\alpha$ emission wavelength to within a few angstroms. From the location of the $H\alpha$ line, a redshift could be calculated and it could be determined if the target was at the right distance to be in the void. The set of filters they were using allowed them to calculate a cz of up to $8,500\text{ km/sec}$. The results of that campaign are still being analyzed, with several promising candidates and follow up spectroscopy work needing to be done to confirm their findings (Moody Provo, UT, Nov. 2013).

It was while pondering on how to improve this method that Dr. Moody developed the idea of using a set of two oppositely sloped, or ramped, filters to effectively do the same thing that the set of three overlapping filters were doing. If the transmission ratios of the two filters could be calibrated to a specific wavelength, and that wavelength could be contrasted with $H\alpha$ 6563\AA wavelength to measure the redshift (assuming that the transmissions are near the $H\alpha$ line).

Since not all galaxies have the same intensity of emissions (for that matter only about 30% of all galaxies have emissions at all), it was also determined that a continuum source would need to be measured in order to normalize and compare the results. It was decided that we would try a $5nm$ red continuum filter for this first round of tests.

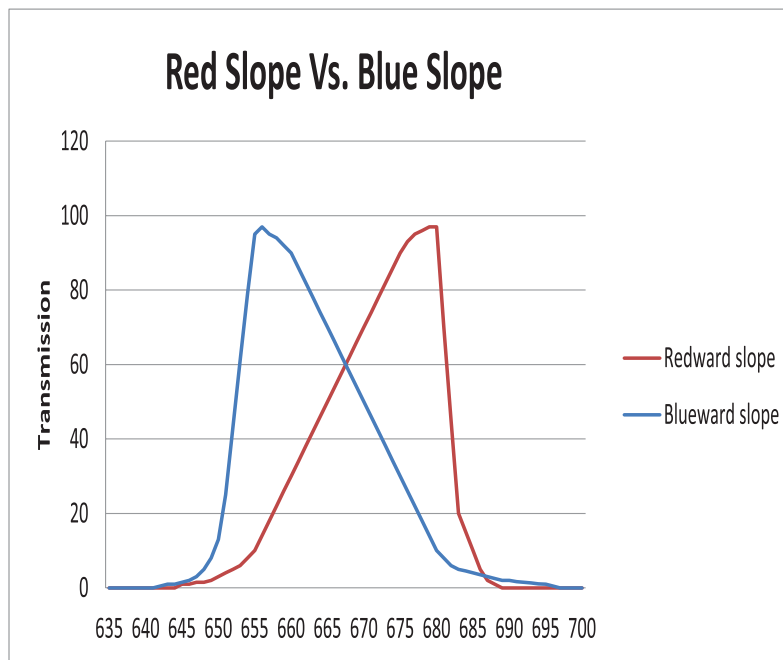


Figure 1.2 The transmissions percentages per wavelength for the red and blue slope filters.

The idea now was that instead of imaging each object through the three overlapping $H\alpha$ filters, one could simply measure the intensity through the two ramp filters and by contrasting those with a measurement through a continuum filter, map the results to a linear relationship with the known redshift values.

1.3 Redshift Fitting Model

The true challenge in analyzing the data is trying to understand the response of the targets to the slope filters and to understand how to use the transmissions with the continuum to get a redshifted wavelength. This can be accomplished as follows:

The continuum intensity would be proportional to the intensity through the continuum filter divided by the filter width

$$I_c = I_{rc} / \Delta\lambda_{rc} \quad (1.2)$$

. The intensity through the blue slope filter would be equal to the continuum intensity multiplied by the slope filter width divided by 2, plus the change in the intensity of the $H\alpha$ line due to the shift in the wavelengths measured from the start of the bandpass

$$I_{bs} = \frac{I_c \Delta\lambda_{slope}}{2} + I_{H\alpha} \left(1 - \frac{\lambda_0 - \lambda_{start}}{\Delta\lambda_{slope}}\right) \quad (1.3)$$

, where λ_0 is the redshifted wavelength. The intensity through the red slope filter being similar, but measuring the $H\alpha$ shift from the end of the bandpass

$$I_{rs} = \frac{I_c \Delta\lambda_{slope}}{2} + I_{H\alpha} \left(1 - \frac{\lambda_{end} - \lambda_0}{\Delta\lambda_{slope}}\right) \quad (1.4)$$

. From there, letting

$$\varepsilon = \frac{I_c \Delta\lambda_{slope}}{2} \quad (1.5)$$

, we can say that

$$I_{H\alpha} = \left(\frac{I_{bs} - \varepsilon}{\Delta\lambda_{slope} - \lambda_0 + \lambda_{start}}\right) \Delta\lambda_{slope} = \Delta\lambda_{slope} \left(\frac{I_{bs} - \varepsilon}{\lambda_{end} - \lambda_0}\right) \quad (1.6)$$

. Thus

$$I_{rs} = \varepsilon + \Delta\lambda_{slope} \left(\frac{I_{bs} - \varepsilon}{\lambda_{end} - \lambda_0}\right) \left(1 - \frac{\lambda_{end} - \lambda_0}{\Delta\lambda_{slope}}\right) = \varepsilon + \left(\frac{I_{bs} - \varepsilon}{\lambda_{end} - \lambda_0}\right) (\Delta\lambda_{slope} - \lambda_{end} - \lambda_0) \quad (1.7)$$

. Thus

$$(I_{rs} - \varepsilon)(\lambda_{end} - \lambda_0) = (I_{bs} - \varepsilon)(\lambda_0 - \lambda_{start}) \quad (1.8)$$

, and

$$\lambda_0((I_{bs} - \varepsilon) + (I_{rs} - \varepsilon)) = \lambda_{end}(I_{rs} - \varepsilon) + \lambda_{start}(I_{bs} - \varepsilon) \quad (1.9)$$

, from which we arrive at the Moody-Holden-McNeff relation,

$$\lambda_0 = \frac{\lambda_{end}(I_{rs} - \varepsilon) + \lambda_{start}(I_{bs} - \varepsilon)}{I_{bs} + I_{rs} - 2\varepsilon} \quad (1.10)$$

.

Which λ_0 we can then compare to the $H\alpha$ wavelength in order to measure the z values of each of the targets.

Chapter 2

Observing and Implementation

2.1 Instrumentation

The slope filters were designed for a transmission range of 6520Å to 6830Å. The Blue Slope filter has transmission values such that maximum percentage, 97% occurs at 6550Å with, 90% @ 6600Å, 80% @ 6650Å, 70% @ 6700Å, 60% @ 6750Å; , 50% @ 6800Å and, so on in a linear fashion until it gets to 0%.

The Red Slope filter is the exact mirror with transmissions of 50% @ 6550Å , 60% @ 6600Å , 70% @ 6650Å , 80% @ 6700Å , 90% @ 6750Å , with maximum percentage (97%) occurring 6800Å. The filters were produced by the Newport Corporation, located in Franklin, Massachusetts.

The telescope that was selected for the trial of this technique was the Remote Observatory for Variable Object Research (ROVOR) that is run by Brigham Young University on donated land in Delta, Utah. ROVOR has been a fully-functioning remote observatory since 2008, producing data mainly for AGN and Gamma Ray Burst research. ROVOR has been a part of several large publica-

tions as well as multiple undergraduate senior theses (see <http://rovor.byu.edu/publications>). The site is equipped with a 16" RC optical tube set up on an a Software Bisque Paramount ME German Equatorial Mount. The CCD is a 1kx1k Apogee Ap8 camera in a Finger Lakes Instrumentation (FLI) body and gives 1.35 arcsec pixel resolution and a 22x22 arcminute FOV (Pearson Brigham Young University, Provo, U.T., 2010). The seeing at the sight is not perfect, but fairly stable with a value of about 3.0" (Moody Provo, UT, Sept. 2013).

The Fingerlakes Filter Wheel is equipped for 6 filters. In addition to the two slope filters with the above specifications, we decided to use a 5nm narrow band red continuum filter (see figure 2.1) to give us a continuum reading so we could normalize the slope filter values. The standard Sloan g, r, and i filtes were used in the remaining 3 slots as a potential means of doing some color comparison work. The telescope and equipment were controlled with Software Bisque's SkyX software and all the data was reduced with standard IRAF procedures.

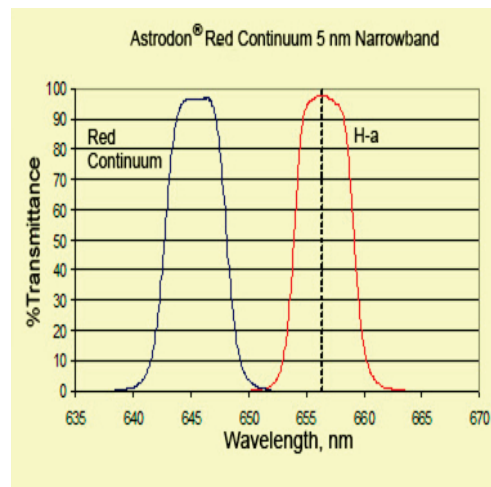


Figure 2.1 The transmissions percentages for the Astrodon 5nm red continuum filter.

Object	R.A.	Dec	cz	$H\alpha$
Mrk 1104	16 05 45.912	+41 20 41.10	2212	133
UGC 7143	12 09 46.714	+25 01 33.83	2545	29
UGC 7040	12 03 53.727	+25 26 02.80	3117	53.6
UGC 4516	08 41 18.230	+66 51 37.24	3992	20
UGC 4376	08 24 53.461	+66 52 10.20	4346	47.6
2MASX J08382309+6507160	08 38 23.093	+65 07 16.05	5728	203
UGC 7277 S	12 15 37.291	+28 10 10.62	6624	15.3
IC 4297	13 35 19.248	+26 25 28.86	7415	17.5
MCG+05-32-056	13 39 44.136	+27 46 35.03	8575	34.1
2MASX J15575804+4147338	15 57 58.048	+41 47 33.85	10362	30.8
NVSS J155636+415250	15 56 36.420	+41 52 50.19	10578	99.9
NGC 5251	13 37 24.855	+27 25 09.76	11161	9.3
MCG+11-11-006	08 29 20.418	+67 10 58.36	11249	24.4

Table 2.1 The list of the target objects with their R.A., Dec. and cz value, and $H\alpha$ equivalent widths in order of lowest to highest cz .

2.2 Targets

Given the specifications of the slope filters, we wanted to select a group of target galaxies roughly within the range of $cz = 2000$ to $cz = 10,000$. These targets were selected from a list of galaxies, whose spectral work had already been done, near the constellation of Bootes (Moody University of Michigan, Ann Arbor, M.I., 1986). The specific targets were selected because of their location within the desired cz range and their favorable position in the sky. Table 2.1 has the list of the targets, their RA and Dec, measured cz , and the equivalent width of their $H\alpha$ line.

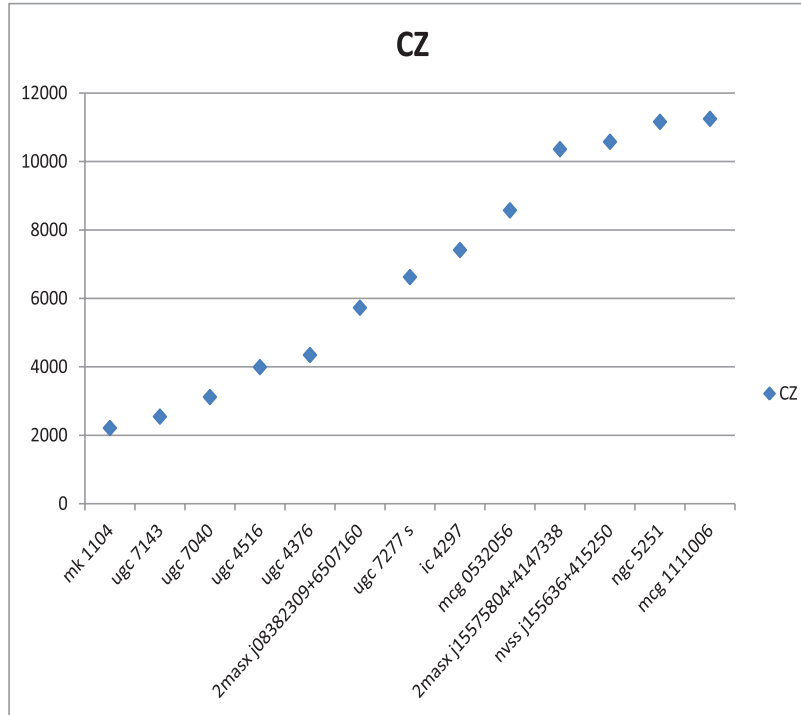


Figure 2.2 Plot of Target Objects in list of Ascending redshift

2.3 Observing

Due to the time involved in producing the slope filters, major hardware and software upgrades to the telescope (and the debugging process therein involved), communication problems with an internet provider, and several other setbacks, what had been planned as a several month campaign was reduced to just a few weeks. During the months of May and June 2014 we were able to take 5

nights of data using the slope filters, with each night being dedicated to half of the targets. Those nights were May 12th, 13th and 14th, and July 1st and 5th.

Each night, the observations were preceded by taking flat frames in as many of the filters as could be reliably done, and dark and bias frames were also taken as it became appropriately dark. These frames were used in the reduction process specifically for each night that they were taken.

We used a palindrome pattern for imaging each target, with 3 two-minute exposures for both of the slope filters, 5 two-minute exposures for the red continuum filter and 3 one-minute exposures for each of the g , r , and i Sloan filters. Next starting in reverse order and keeping same exposure times we went through the filters again, ending on the red slope filter.

One of the wonderful advantages of using a remote robotic telescope like ROVOR is that there is no need to have someone continually monitoring the telescope as it runs. But that also means that not all of the errors are caught as they are taking place. A few weeks after we began the run, we discovered that a scripting bug was causing the telescope to occasionally take a bias frame in place of the light and dark frames. In addition to this, it was discovered that during several of the nights there was some significant interference with high cirrous clouds, resulting in several of the targets have data missing from one or more of the filters.

2.4 Data Reduction

The data was reduced through standard IRAF procedures with bias and dark subtraction, and flat fielding with the appropriate filter flat frame. If the flat frame for a given filter was not taken dur-

ing the night from which the data was being processed, then flat frames from the nearest night of observing were used in its place.

Each frame was then analyzed using the program NightPhot4, and then the resulting data (i.e. magnitudes, flux) for each object was averaged for each of the filters per object per night. In particular it should be noted that for many of the red continuum filter frames, the signal to noise was so poor that it became difficult to confidently measure. The best that could be done was effectively tried, but this remains a source of error in the final results.

Chapter 3

Results

3.1 Data

The initial results analyzed were those of the magnitudes for each of the targets through each filter. Figures 3.1-3.3 show the telescopic apparent magnitude for each target that was captured for each series of nights. The ordering of the targets in each of the plots is from the smallest redshift to the largest. Similar plots showed the same results for the measurements of the flux for each filter. At first glance the data was encouraging in that it looked like there might be a possible correlation between the redshift and the ratio of the blue filter and red filter magnitudes.

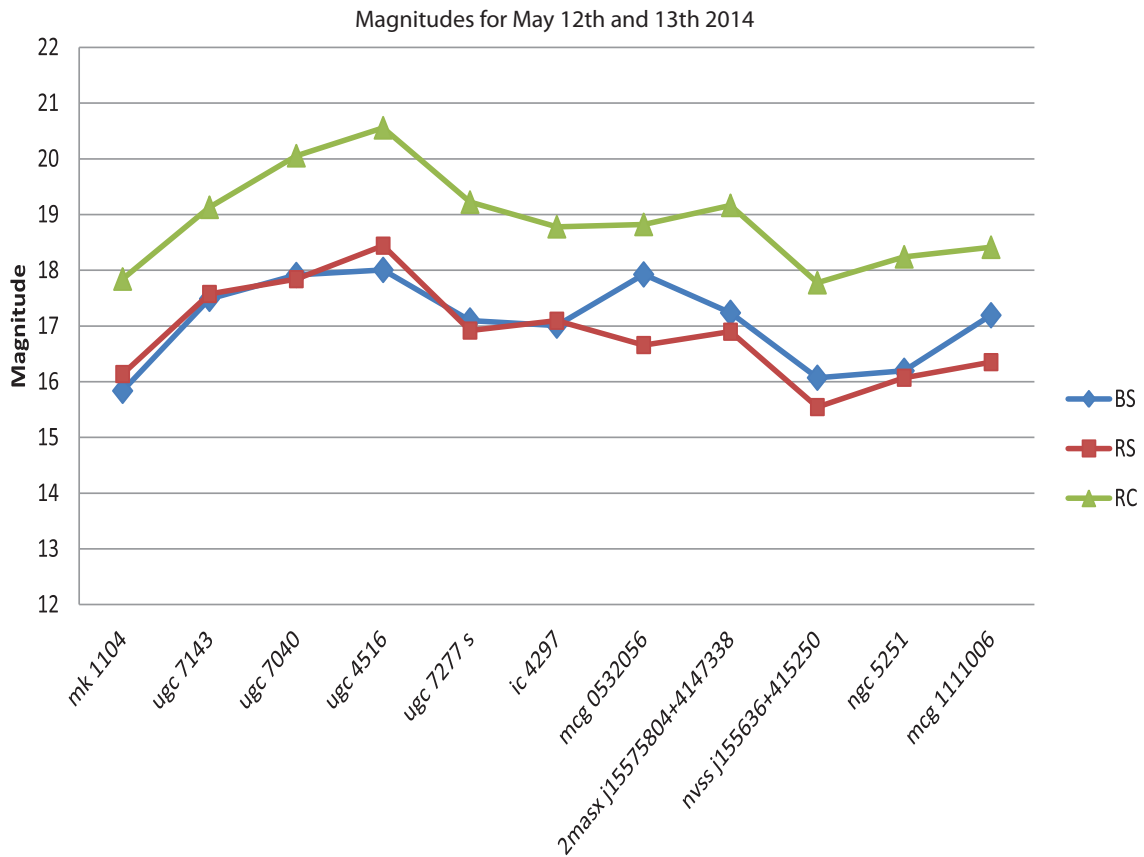


Figure 3.1 Magnitudes of the slope and continuum Filters for the Nights of May 12th and 13th

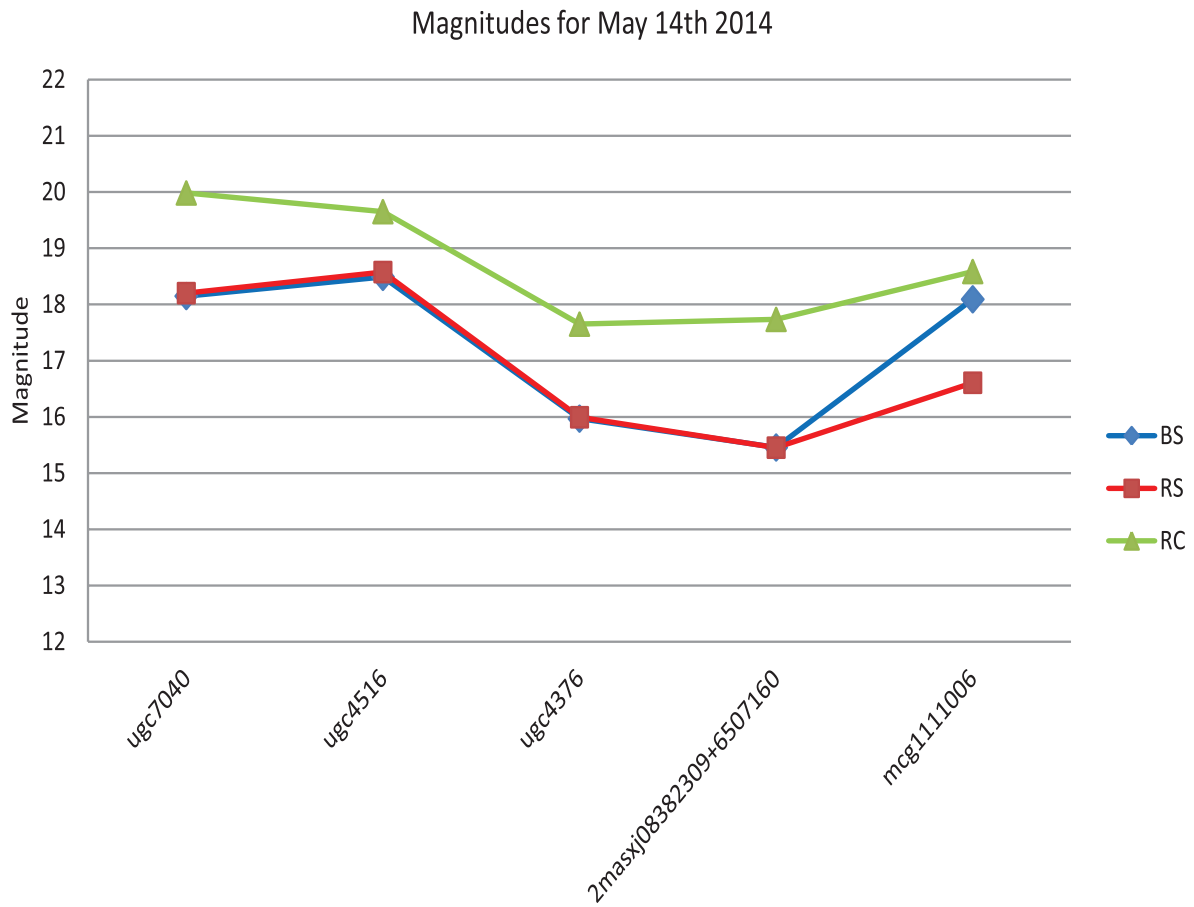


Figure 3.2 Magnitudes of the slope and continuum Filters for the Night of May 14th

Upon closer examination, we realized that there was a large amount of scatter in the counts of many of the targets throughout the runs. For example, on May 12th, *UGC* 7143 went from 1800 counts in the red slope filter, down to 500 in a little over an hour. While not all the data was this extreme, it tended to be more the exception than the rule to have a stable transmission over the hour the telescope was focused on a target. With that being said, we did seem to get some relatively good and stable conditions for 2Masx J083, and MCG 05. Nonetheless, the purpose of the work was to test the method in general, so having some instability in the counts allowed us to test the robustness of the method as well.

Also it should be noted that the last two targets, NGC 5251 and MCG+11-11-006, are both near the theoretical edge of what the filters should be able to detect. Thus their results, for good or bad, should be taken with a grain of salt.

3.2 Fit Vs. Real CZ

When it came time to employ the Moody-Holden-McNeff relation (MHM relation) to solve for the λ_0 , and thus the redshift, several different approaches were taken in order to find the best fit (due to the lack of quality data).

3.2.1 Straight Count Averages

Initially the MHM relation was employed by simply averaging the fluxes in each filter, scatter and all, and putting the values in for I_{rc} , I_{bs} , and I_{rs} into the relation. The results are summarized in Figures 3.4-3.8 and Table 3.1.

Object	Real Z	May 12th	May 13th	May 14th	July 1st	July 5th
Mrk 1104	0.007373	-	0.01118	-	0.01875	-
UGC 7143	0.008483	0.01901	-	0.02522	-	-
UGC 7040	0.01039	0.01802	-	0.01685	-	-
UGC 4516	0.01330	0.03151	-	0.04536	-	0.01905
UGC 4376	0.01448	0.03198	-	0.01684	-	0.02969
2MASX J08382309+6507160	0.01909	0.03371	-	0.02268	-	0.02002
UGC 7277 S	0.02208	0.02221	-	-	-	-
IC 4297	0.02471	-	0.01866	-	0.01982	-
MCG+05-32-056	0.02858	-	0.05376	-	0.01934	-
2MASX J15575804+4147338	0.03454	-	0.02377	-	0.03500	-
NVSS J155636+415250	0.03526	-	0.02785	-	0.02376	-
NGC 5251	0.0372	-	0.01980	-	0.01294	-
MCG+11-11-006	0.03749	0.04002	-	0.06273	-	0.02521

Table 3.1 The list of the target objects with their true z value and estimated z value for the various nights, in order of lowest to highest z .

As can be seen, there is a lot of scatter between the various nights. This is a pretty good indication that the nights, though forecast to be clear, did in fact have some cloudy interference. That being said, each of the targets had at least one point through the 5 nights that was relatively close to what the actual z value should be. There also appeared to be a generally good linear fit, albeit with several large outliers. Unfortunately, the signal to noise for the red continuum filter was often very poor, often not exceeding the sky background counts, putting into question the reliability of the data.

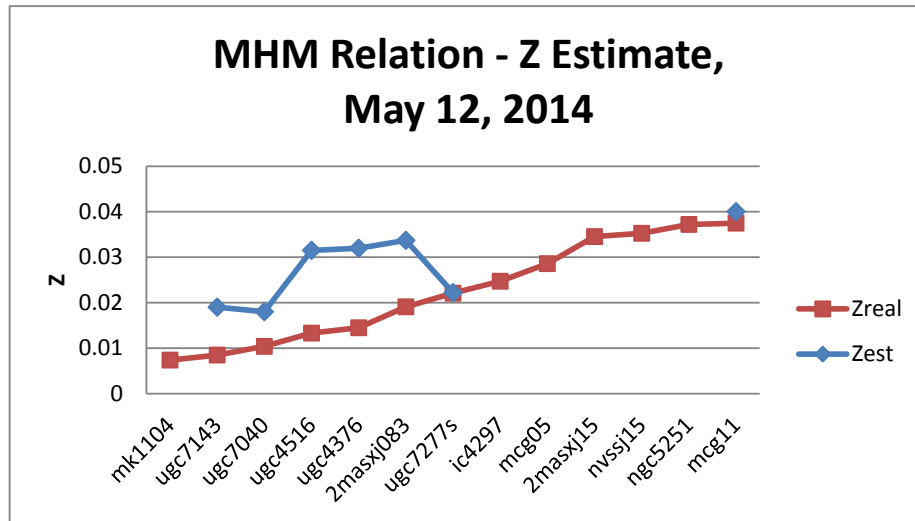


Figure 3.4 Z estimate compared with the actual Z values for the night of May 12

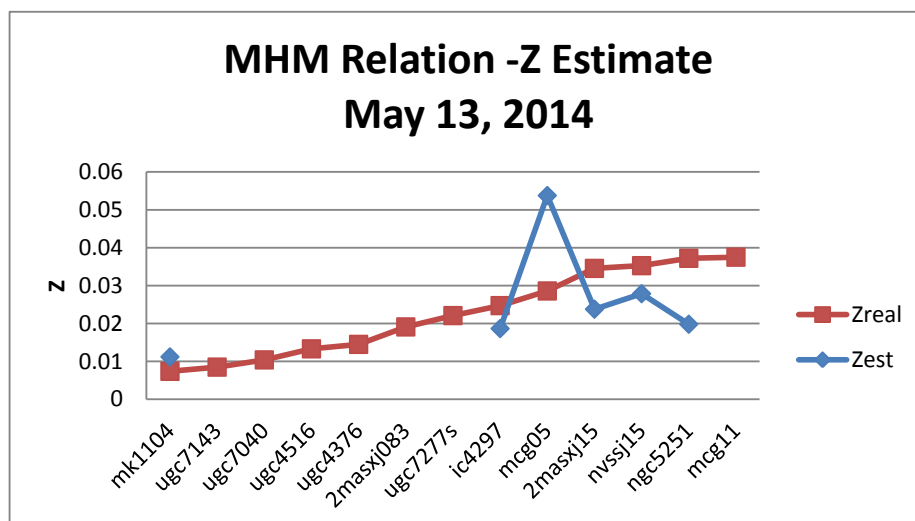


Figure 3.5 Z estimate compared with the actual Z values for the night of May 13

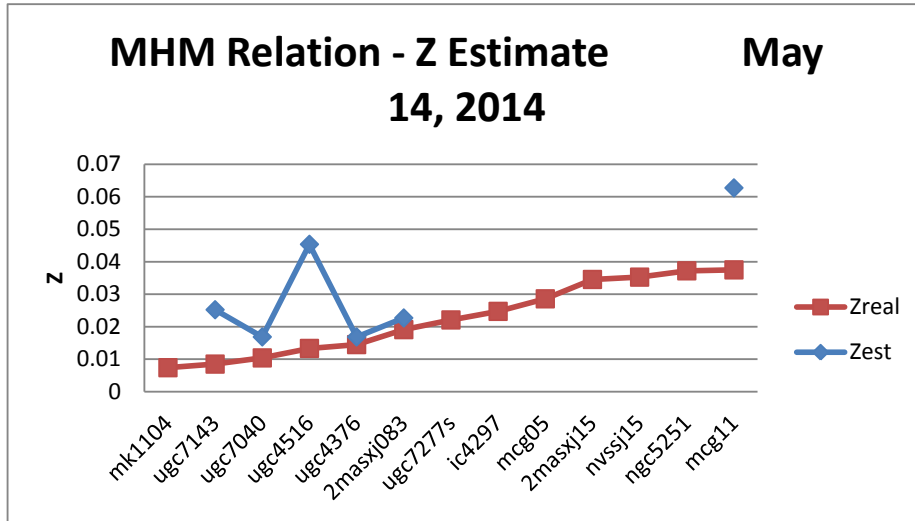


Figure 3.6 Z estimate compared with the actual Z values for the night of May 14

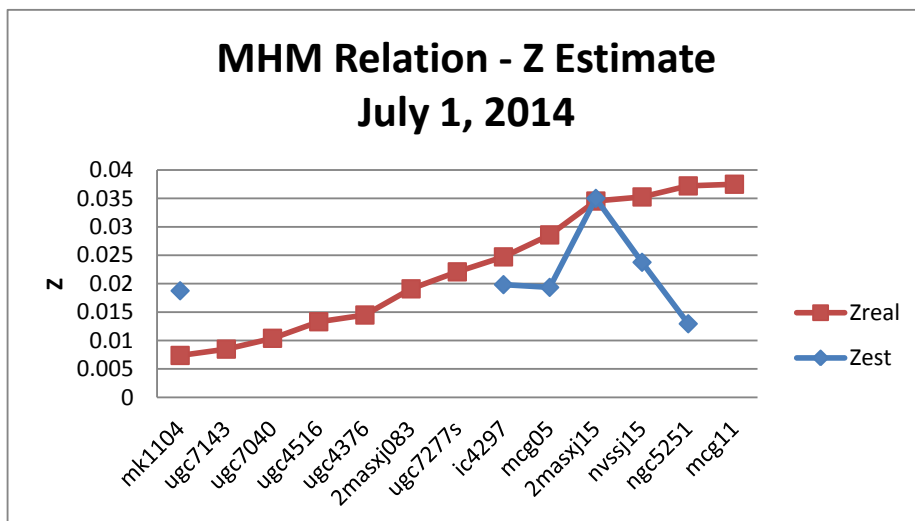


Figure 3.7 Z estimate compared with the actual Z values for the night of July 1

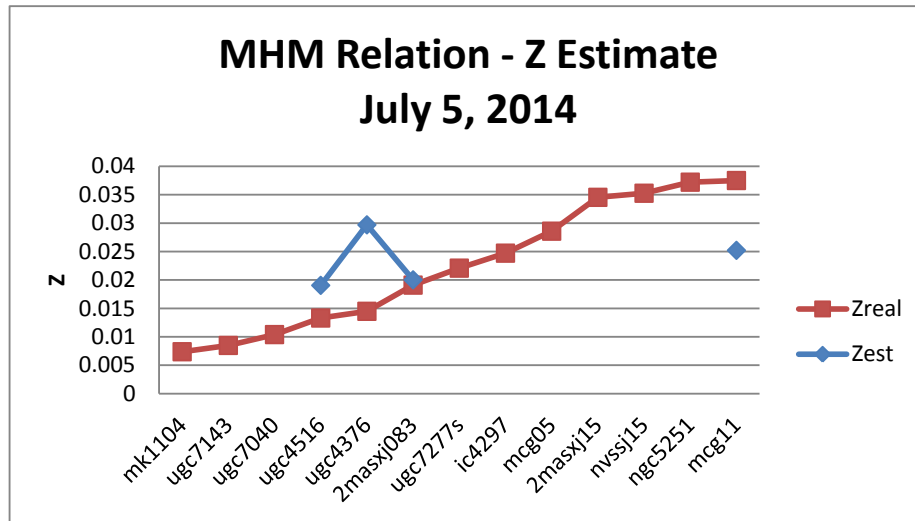


Figure 3.8 Z estimate compared with the actual Z values for the night of July 5

3.2.2 Noise Revision

In an attempt to clear up some of the noise, I went through the data for each of the nights and removed the obviously cloud-influenced data (i.e. the blue slope filter going from 1800 counts to 300 counts within an hour). Then I recalculated all the averages and the redshifts. I called this the revised redshift counts and they are summarized in Table 3.2 and Figures 3.9-3.13. It is interesting to note that while this approach significantly improved the estimated z for several of the targets, it also made some of them worse. It is possible that the cloud interference came and went in a such a fashion, that while the counts seemed stable, they were repressed, so that by "cleaning up" one of the other filters caused the ratios to be worse than they were before.

Object	Real Z	May 12th	May 13th	May 14th	July 1st	July 5th
Mrk 1104	0.007373	-	0.01487	-	0.01578	-
UGC 7143	0.008483	0.01940	-	0.02522	-	-
UGC 7040	0.01039	0.01364	-	0.03148	-	-
UGC 4516	0.01330	0.02903	-	0.05315	-	0.01515
UGC 4376	0.01448	0.03692	-	0.01961	-	0.02568
2MASX J08382309+6507160	0.01909	0.03250	-	0.02512	-	0.01932
UGC 7277 S	0.02208	0.03376	-	-	-	-
IC 4297	0.02471	-	0.02883	-	0.01983	-
MCG+05-32-056	0.02858	-	0.05700	-	0.01994	-
2MASX J15575804+4147338	0.03454	-	0.02565	-	0.02662	-
NVSS J155636+415250	0.03526	-	0.02785	-	0.02445	-
NGC 5251	0.0372	-	0.02020	-	0.01709	-
MCG+11-11-006	0.03749	0.04101	-	0.03460	-	0.02694

Table 3.2 Revised list of the target objects with their true z value and revised estimated z value (removing the cloud affected data) for the various nights, in order of lowest to highest z.

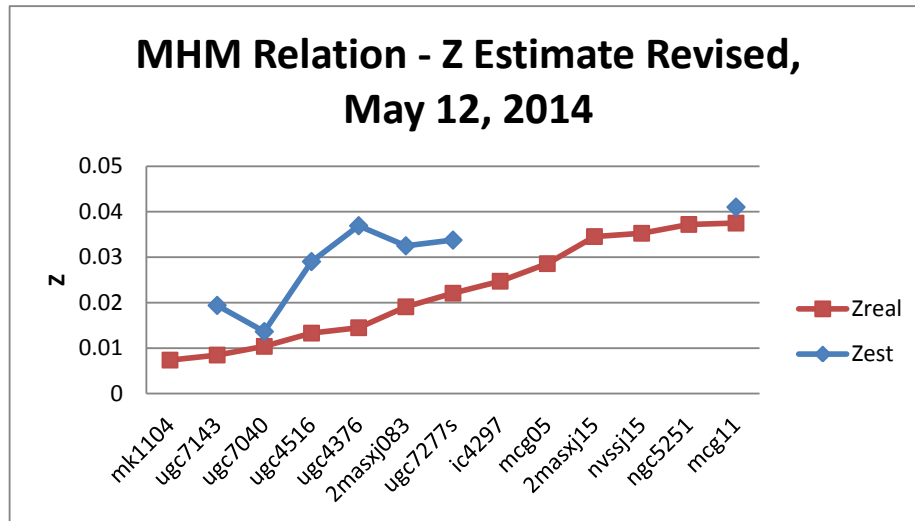


Figure 3.9 Z estimate compared with the actual Z values for the night of May 12

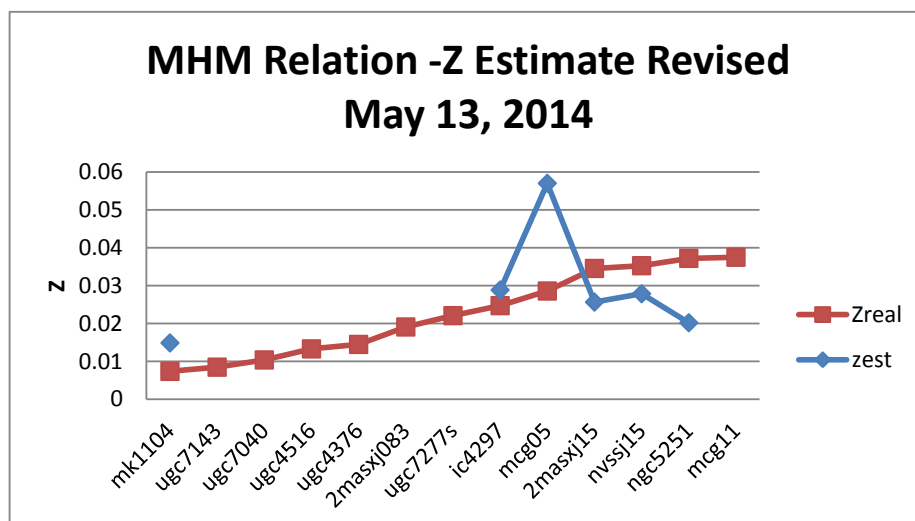


Figure 3.10 Z estimate compared with the actual Z values for the night of May 13

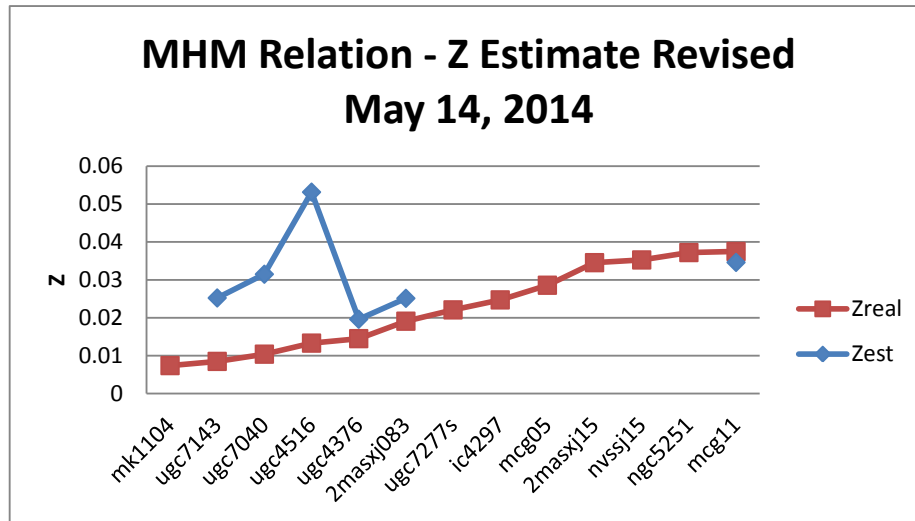


Figure 3.11 Z estimate compared with the actual Z values for the night of May 14

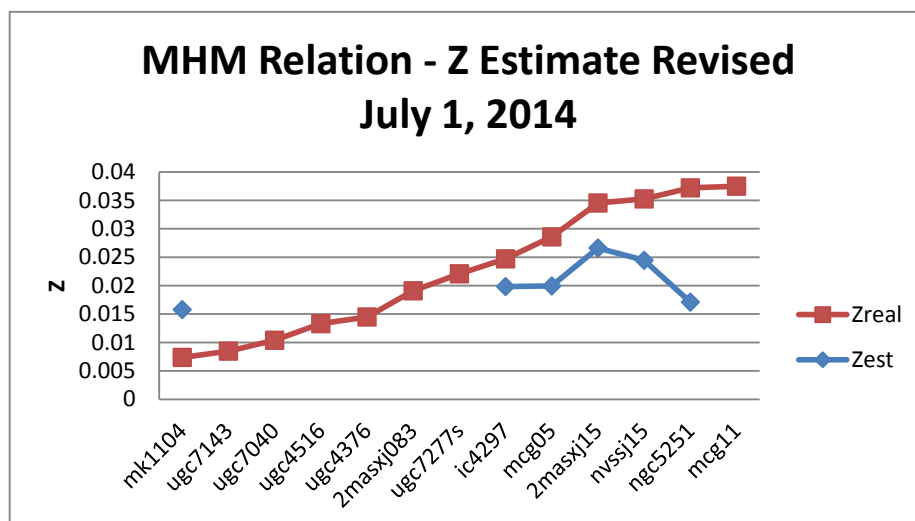


Figure 3.12 Z estimate compared with the actual Z values for the night of July 1

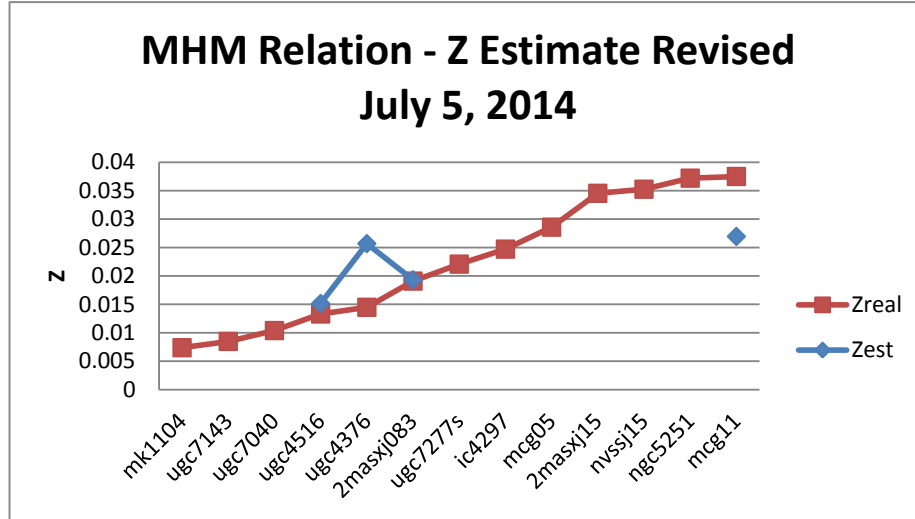


Figure 3.13 Z estimate compared with the actual Z values for the night of July 5

3.2.3 Changing the Continuum

Given that the signal to noise for the red continuum filter was fairly poor, an idea was put forth to try using the slope filters themselves to measure the continuum. In the original selection of the targets, we looked not only for galaxies with a range of redshifts but also with a range of emission in $H\alpha$. Using the $H\alpha$ equivalent widths (see Table 2.1), we set the new intensity of the continuum equal to the intensity of the blue slope plus the intensity of the red slope, divided by the width of the filters added to the equivalent width. Thus we could get an idea for the counts per angstrom.

So

$$I_{cnew} = \frac{I_{bs} + I_{rs}}{\Delta\lambda_{slope} + H\alpha} \quad (3.1)$$

, with a new ϵ

$$\epsilon = \frac{310 * I_{cnew}}{2} \quad (3.2)$$

Using this new model we recalculated all the redshifts for the 5 nights of the revised data. In general the values were worse, but it still appeared to be trending in the right direction.

This method, of course, would not be employable in the grand scheme of doing galactic surveying due to the fact that we would have no idea what the equivalent widths would be for the majority of the galaxies being examined. But for the course of initial calibration and modeling that we are undertaking here, the theory works just fine.

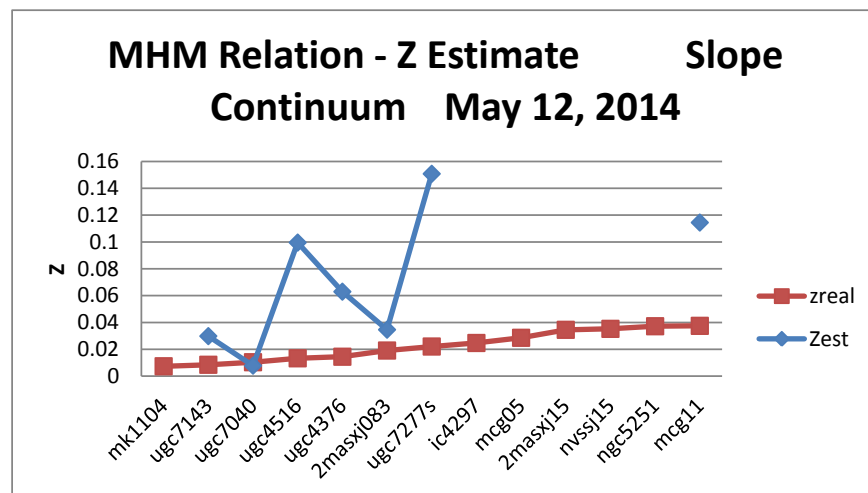


Figure 3.14 Z estimate compared with the actual Z values for the night of May 12, with the slope filters for the continuum.

Object	Real Z	May 12th	May 13th	May 14th	July 1st	July 5th
Mrk 1104	0.007373	-	0.01302	-	0.02395	-
UGC 7143	0.008483	0.02982	-	0.1124	-	-
UGC 7040	0.01039	0.007836	-	0.04576	-	-
UGC 4516	0.01330	0.09954	-	0.1392	-	0.03221
UGC 4376	0.01448	0.06294	-	0.02448	-	0.03365
2MASX J08382309+6507160	0.01909	0.03462	-	0.02558	-	0.01998
UGC 7277 S	0.02208	0.1507	-	-	-	-
IC 4297	0.02471	-	0.1162	-	0.03824	-
MCG+05-32-056	0.02858	-	0.1217	-	0.02992	-
2MASX J15575804+4147338	0.03454	-	0.07758	-	0.0724	-
NVSS J155636+415250	0.03526	-	0.04008	-	0.02984	-
NGC 5251	0.0372	-	0.06366	-	0.01740	-
MCG+11-11-006	0.03749	0.1144	-	0.09602	-	0.05120

Table 3.3 List of the target objects with their true z value and estimated z value using the new I_{new} and ϵ (using the slope filters for the continuum) for the various nights, in order of lowest to highest z.

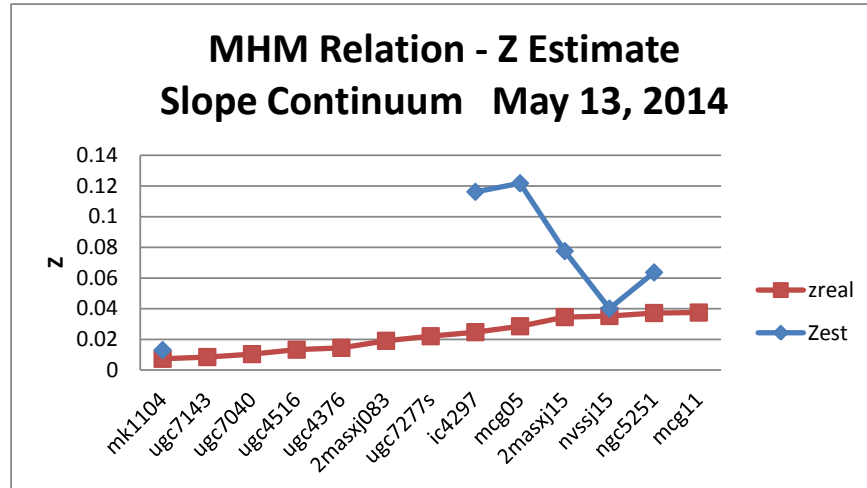


Figure 3.15 Z estimate compared with the actual Z values for the night of May 13, with the slope filters for the continuum.

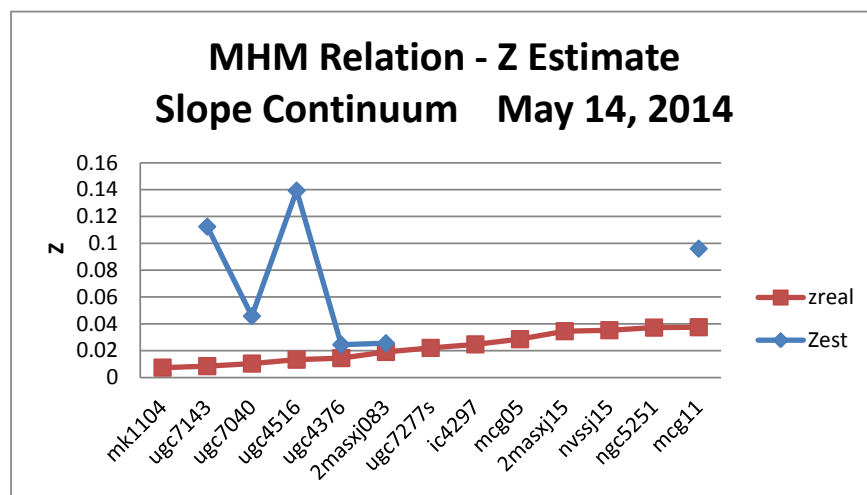


Figure 3.16 Z estimate compared with the actual Z values for the night of May 14, with the slope filters for the continuum.

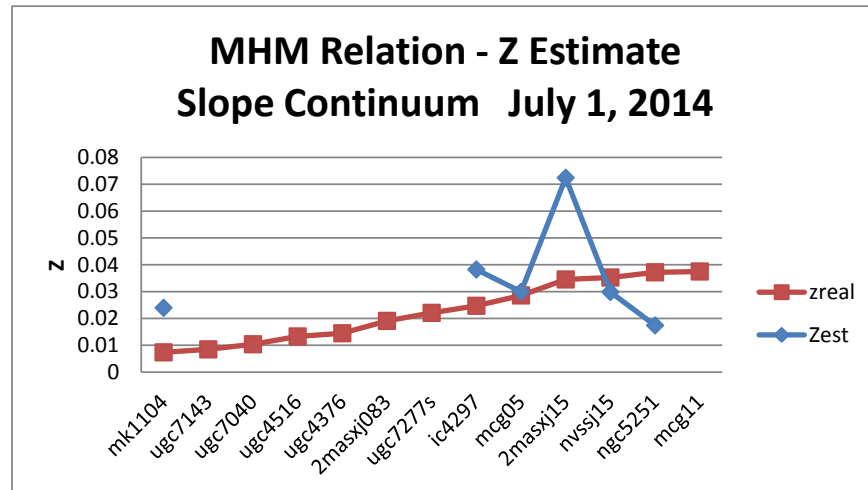


Figure 3.17 Z estimate compared with the actual Z values for the night of July 1, with the slope filters for the continuum.

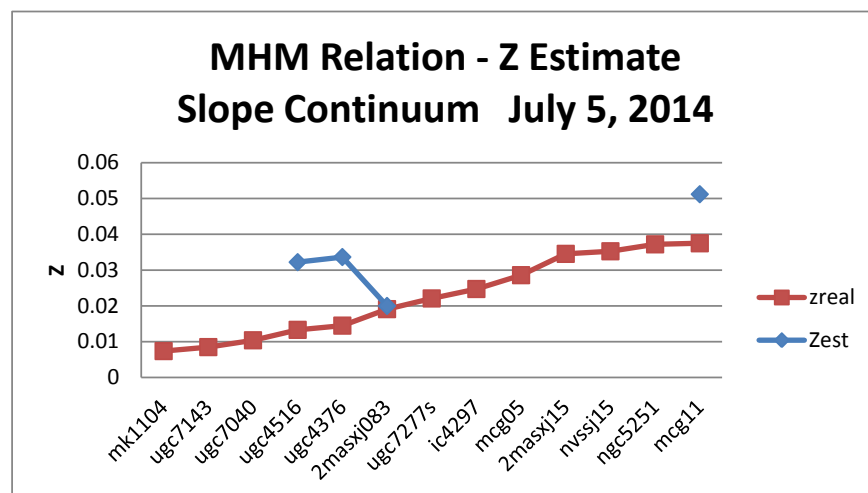


Figure 3.18 Z estimate compared with the actual Z values for the night of July 5, with the slope filters for the continuum.

Object	Real Z	May 13th Sloan g	May 13th Sloan i
Mrk 1104	0.007373	0.01436	0.01396
IC 4297	0.02471	0.01766	0.01784
MCG+05-32-056	0.02858	0.02897	0.03003
2MASX J15575804+4147338	0.03454	0.02088	0.02066
NVSS J155636+415250	0.03526	0.01974	0.01972
NGC 5251	0.0372	0.01837	0.01858

Table 3.4 List of the objects in ascending Z order, for the night of May 13, using the Sloan g and i filters for the continuum

3.2.4 Other Continuum

As previously stated, data was also collected on all of the targets in the Sloan g,r and i filters. We decided to take a look at the data using the g and i filters as a measure of the continuum instead of the slope filters or the red continuum filter. The only difference in the derivations would be the use of those individual filter widths and their flux, in place of the red continuum flux and filter width. We only applied the method to the night of May 13, due to the fact that it had the most consistent number of the Sloan filter frames, between all the targets, in comparison to the other nights. The results are summarized in Table 3.4 and Figure 3.19.

Overall it seemed like using the Sloan filters for the continuum measurement was not a bad estimate, as it tightened some of the spread when compared to the red continuum and slope continuum methods.

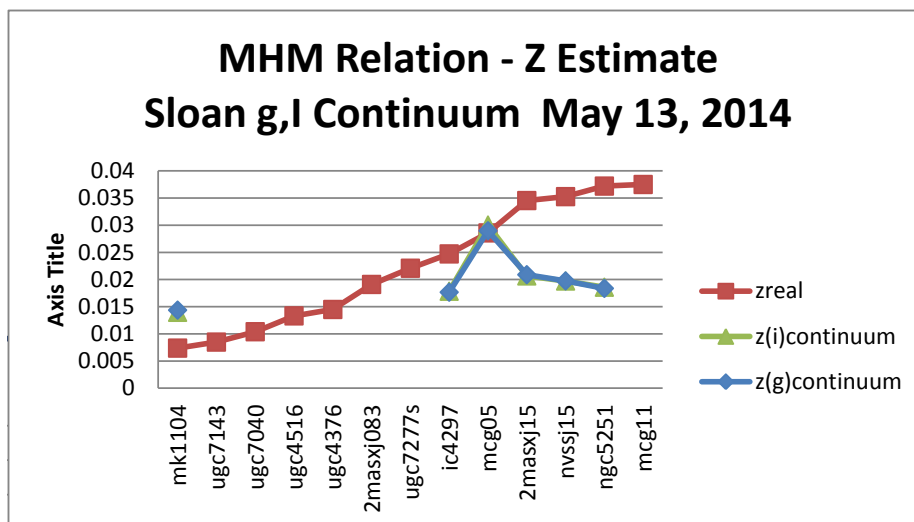


Figure 3.19 Z estimate compared with the actual Z values for the night of July 13, with the Sloan g and i filters for the continuum.

3.2.5 Closest Point Method

Despite the poor data we had, due to the degradation of the frames by clouds, there were several points for each of the targets that seemed to be very near the correct redshift. In fact if we take the red continuum method and take the closest point out of all the nights for each target (from table 3.1), we get a plot like Figure 3.20.

I have removed the last two data points from Figure 3.20, because they are on the theoretical edge of what can be measured with the filters, and because they have the least accurate measurements from this particular set. The results are very close to what we were looking for, and if we assume that these were the observations made during the clearest moments for each target, it sug-

gests the method is working.

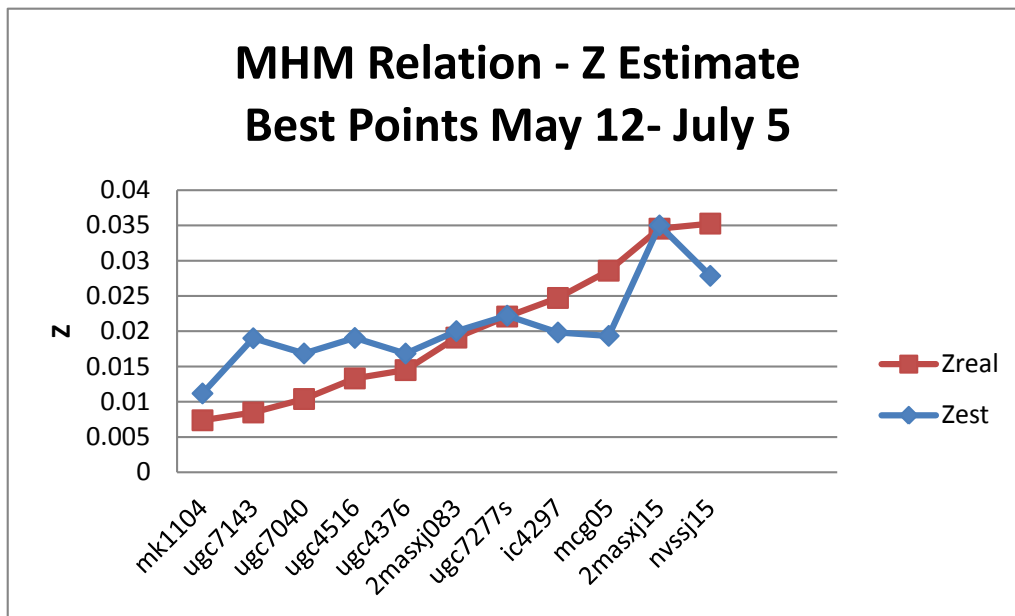


Figure 3.20 Z value comparison with the best points over the 5 nights of observation from May 12 - July 5th.

Chapter 4

Conclusions

4.1 Discussion

In considering the results, it is most importantly noted that this work needs to be done on photometric nights. Despite the fact that there seems to be a general trend following the real Z slope for all of our different methods of analysis, the data is just too degraded by clouds to be able to make any conclusive arguments. The poor signal to noise in the red continuum filter and the lack of quality frames for the Sloan filters, (seemed to be caused some bug in the process) make it so we can't truly compare the two methods. Additionally the cloud interference makes it impossible to really trust the results from using the slope filters for the continuum either.

The closest point method seems to be the best choice when it comes dealing with non-photometric data. It was very near where we wanted to be, and is a decent statistical method to account for the cloud degradation. In fact, if you also apply closest point method to the slope continuum results (Table 3.3), you will notice that even though the estimates are not as close to the true z values as they are for the red continuum results (Table 3.1), 10 out of the 11 nights correlate as for which

was the best night of observing for each target. This lends credence to the idea that those particular windows of observation were the least cloudy for each target.

Even with those results, conclusions made have to be slightly suspect given the non-uniformity of the data. Part of this research project was to test the hardiness of the method and see what its limits were. The results show that the method has great promise for working, but that it is a process that should be saved for strictly photometric nights.

It also seems that while the continuum counts make a difference, it appears that there are several ways that to measure it. Each method tried here seemed to lead to the same general trend despite the changes in the estimated z values. It did seem that the greater signal to noise of the Sloan filters made a difference in improving the data. It would remain for future work to see if one filter is better than another.

4.2 Future Work

Again, this is data that needs to be collected on photometric nights to be truly understood. Also, the better the signal to noise, the better the results should be. Thus the current plan is to move this project from ROVOR to the West Mountain Observatory 20" telescope.

It is interesting to note that in all of the analysis methods, for targets on the left half of the plot, the estimated Z value is high; while on the right half of the plot the estimated Z value is low. It seems the two halves of the data almost mirror each other as well, especially if you look at the hodgepodge of the closest point method data set in Figure 3.20. This may be something that

needs to be corrected for, such that the farther away you get from the center, the higher the needed correction is going to be. But again, this is something that will need to be checked when an better quality data set is obtained.

The ultimate goal for this project has always been to enable a small telescope like ROVOR to take part in a deep survey of galactic voids. If the MHM relationship is verified through further research, this method could lead to a revolutionizing understanding of what, up to now, is only known as empty space.

Bibliography

J. Moody, e. a. 2012, Publications of the Astronomical Society of the Pacific, 124, 866

Moody, J. University of Michigan, Ann Arbor, M.I., 1986, Ph.D. dissertation

Moody, J. W. Provo, UT, Nov. 2013, presented at the BYU Physics Colloquium during Fall Semester of 2013,

—. Provo, UT, Sept. 2013, NSF Grant Proposal

Pearson, R. Brigham Young University, Provo, U.T., 2010, B.S. Senior Thesis

R. Ellis, e. a. 2013, The Astrophysical Journal Letters, 763, 1

Ryden, B., & Peterson, B. 2010, Foundations of Astrophysics, 1st edn., ed. N. Whilton (1201 Sansome St., San Francisco, CA 94111: Pearson Addison-Wesley), 484

S.Barden, J.Arns, & W.Colburn. 1988, Proc. SPIE, 3355, 866